

Magnetotransport Properties in Epitaxial Exchange-Biased $\text{La}_{2/3}\text{Ca}_{1/3}\text{MnO}_3/\text{La}_{1/3}\text{Ca}_{2/3}\text{MnO}_3$ Superlattices

M. E. Gómez¹, G. Campillo¹, J.-G. Ramírez¹, P. Prieto¹, A. Hoffmann², J. Guimpel³, N. Haberkorn³, A. Condo³,
and F. Lovey³

¹Excellence Center for Novel Materials, Department of Physics,

Universidad del Valle, Ciudad Universitaria Meléndez, A. A. 25360 Cali, Colombia

²Argonne National Laboratory, Materials Science Division and Center for Nanoscale Materials, Argonne, IL 60439 USA

³Centro Atómico Bariloche & Instituto Balseiro, Comisión Nacional de Energía Atómica
& Universidad Nacional de Cuyo, (8400) Bariloche, Argentina

Superlattices of ferromagnetic (F) and antiferromagnetic (AF) oxide materials have attracted increased attention given the *exchange bias* or *exchange anisotropy* phenomenon. Research on magnetic oxide superlattices has focused toward the technological goals of increasing magnetoresistance in lower applied magnetic fields and more useful temperature ranges for various applications. Superlattices of F-LCMO and AF-LCMO layers were grown on (001)-oriented SrTiO_3 substrates. We studied the temperature dependence of magnetotransport properties for a series of $[\text{AF-LCMO}(7.6\text{ nm})/\text{F-LCMO}(t_F)]_N$ superlattices as a function of the ferromagnetically doped layer thickness, t_F , while the antiferromagnetic (AF) layer thickness, t_{AF} , was kept constant. Magnetotransport measurements at different temperatures were done on a series of $[\text{AF}(7.6\text{ nm})/\text{F}(t_F)]_N$ superlattices. The ZFC resistance has a maximum at negative fields, for all multilayers, with descending fields (from 1 to -1 kOe). In all samples a shift along the field axis of the FC loop with respect to that of the ZFC loop is observed. The H_{ex} values determined from these displacements of the FC loops of the magnetoresistance loops increase when temperature decreases and its magnitude also depends on the ferromagnetic layer thickness.

Index Terms—Exchange interactions, interface magnetism, magnetic anisotropy, magnetic multilayers, magnetoresistance, sputter deposition, transmission electron microscopy, X-ray diffraction.

I. INTRODUCTION

WHEN two magnetically different materials are in atomic contact, new and exciting magnetic properties are generated. Since the last decade, especially, there has been renewed interest in the study of so-called magnetic multilayers, consisting of alternating magnetic and nonmagnetic or ferro- and antiferromagnetic layers. Currently, this has also led to intense theoretical and experimental work on the study of coupling mechanisms involved at the interfaces of these systems [1]. In modern applications, the key to modifying and controlling magnetic properties is based on the design of magnetic structures with properties governed by the interface region. Recently, exchange coupling, exchange biasing, and novel magnetic structures have been investigated in epitaxial oxide multilayers comprised primarily of ferro-/paramagnetic, ferro-/antiferromagnetic, and antiferro-/antiferromagnetic materials. The energies involved are exchange (magnetic ordering) and anisotropy (preferred orientation). One of the most interesting interfaces is based on a ferromagnet and antiferromagnet system. Since the antiferromagnet has a vanishing net magnetization, its magnetic order is more robust against changes induced by externally applied fields. In such ferromagnetic/antiferromagnetic heterostructures, exchange coupling can produce a stable ferromagnetic order with high anisotropy; this anisotropy is then unidirectional, which is a

characteristic not found in ferromagnets on their own [2], [9]. This phenomenon is known as *exchange bias*, experimentally manifesting itself in a field shift, H_{ex} , of the hysteretic loop along the field axis, due to a preferred magnetization direction, and is typically accompanied by an increase of the coercivity.

The $\text{La}_{1-x}\text{Ca}_x\text{MnO}_3$ system offers rich magnetic behavior depending on its doping x . We chose the stoichiometric ferromagnetic phase $\text{La}_{2/3}\text{Ca}_{1/3}\text{MnO}_3$ (F-LCMO) with a Curie temperature around 260 K, and the corresponding antiferromagnetic phase $\text{La}_{1/3}\text{Ca}_{2/3}\text{MnO}_3$ (AF-LCMO) with a Néel temperature around 260 K. In fact, several properties associated to exchange bias effects have been recently studied in F-LCMO/AF-LCMO multilayers [3].

In this work, we report a study of structural and temperature dependence of magnetotransport properties for a series of exchanged-biased $[\text{AF-LCMO}(7.6\text{ nm})/\text{F-LCMO}(t_F)]_N$ superlattices as a function of the ferromagnetically doped layer thickness, t_F , varied from 1.9 to 7.6 nm, while the antiferromagnetic (AF) layer thickness, t_{AF} , was kept constant at 7.6 nm. The measurement of the field dependence of resistivity was used to explore exchange bias.

II. EXPERIMENT

Superlattice structures of alternating antiferromagnetic insulating $\text{La}_{1/3}\text{Ca}_{2/3}\text{MnO}_3$ and ferromagnetic $\text{La}_{2/3}\text{Ca}_{1/3}\text{MnO}_3$ layers were grown via a high-pressure sputtering process, using sintered targets with stoichiometric $\text{La}_{1/3}\text{Ca}_{2/3}\text{MnO}_3$ and $\text{La}_{2/3}\text{Ca}_{1/3}\text{MnO}_3$ compounds on (001)-oriented SrTiO_3

substrates. During deposition, the substrate temperature was kept constant at 850 °C and an oxygen pressure at 3.5 mbar was maintained, resulting in a constant deposition rate of approximately 1.5 nm/min, for both types of oxides. The thickness of this AF/F bilayer is defined as the modulation of the superstructure, Λ , and it was varied according to F and AF layer thicknesses, t_{AF} and t_F , respectively. Subsequent bilayers were then grown with N repetitions of Λ such that the total superlattice thickness was a chosen constant at around 180 nm. Reliable values of the modulation period, Λ , of sputtered AF/F manganese superlattices was estimated by means of X-ray diffraction (XRD) measurements.

Magneto-transport measurements were carried out using four point probes in a current in plane (CIP) geometry, while applying the magnetic field parallel to the current flow direction. The measurements were taken at zero field cooling (ZFC) and after field cooling (FC) in an applied magnetic field of 1 Tesla. Magnetoresistance isothermal loops were measured in an appropriate field range ($H = \pm 1$ T), at different temperatures, ranging between 15 and 200 K. The magnetotransport measurements were made by using a Quantum Design extraction magnetometer, equipped with a 7-T superconducting solenoid.

For further characterization of our superlattices, high resolution transmission electron microscopy (HRTEM) and atomic force microscopy (AFM) techniques were used. The samples for TEM imaging were prepared in a cross-section geometry, which can yield features on the atomic scale of the layers. It also allows for the study of strain effect in epitaxial thin films, i.e., interface structure.

III. RESULTS AND DISCUSSION

A typical high-angle X-ray diffraction spectrum for a $[La_{1/3}Ca_{2/3}MnO_3(t_{AF})/La_{2/3}Ca_{1/3}MnO_3(t_F)]_N$ multilayer grown on single-crystal (001) SrTiO₃ substrate is shown in Fig. 1. In this spectrum for a $[AF(15 \text{ u.c.})/FM(3 \text{ u.c.})]_{21}$ superlattice the substrate (S) and LCMO (001)-, (002)-, and (003)-Bragg maxima are visible. In addition, the XRD data displays multiple satellite diffraction peaks around the (00 l) reflection of the multilayer (labeled zero order peak), due to the chemical modulation with a Λ periodicity (bilayer thickness). This spectrum reveals that we have a highly textured heterostructure with the c axis perpendicular to the substrate surface, and the coherent AF/F superlattice peak corresponding to the (002) reflection of STO is observed at about 46.5°. From XRD spectra we obtained values for a_{ave} for $t_F = 1.9, 3.8, 5.7,$ and 7.6 nm (corresponding to 5, 10, 15, and 20 u.c., respectively) ranging between 0.377 ± 0.001 nm, for the thinner F layer, to 0.380 ± 0.001 nm, for $t_F = t_{AF}$. We also fitted the measured intensities of the X-ray data by using the SUPREX 9.0 refinement software [4]. Layer thickness fluctuations of about 0.38 nm (1.0 u.c.) for both F and AF layers were obtained. Furthermore, we found no indications of epitaxial mismatch strain as expected from the small lattice mismatch between F and AF layers.

The inset in Fig. 1 displays a high resolution transmission electron microscopy (HR TEM) image for a $[La_{1/3}Ca_{2/3}MnO_3(10 \text{ u.c.})/La_{2/3}Ca_{1/3}MnO_3(30 \text{ u.c.})]_{10}$ superlattice, with

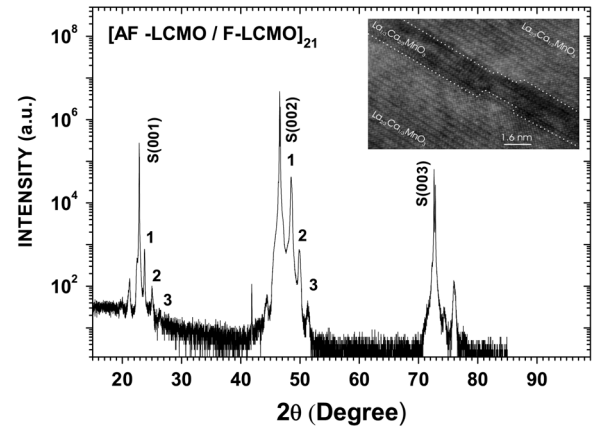


Fig. 1. X-ray diffraction pattern of a $[AF(15 \text{ u.c.})/FM(3 \text{ u.c.})]_{21}$ superlattice. Superlattice peaks are seen adjacent to the main multilayer peak (zero order). Inset shows a TEM image of a $[AF(10 \text{ u.c.})/F(30 \text{ u.c.})]_{10}$ superlattice with atomic plane resolution.

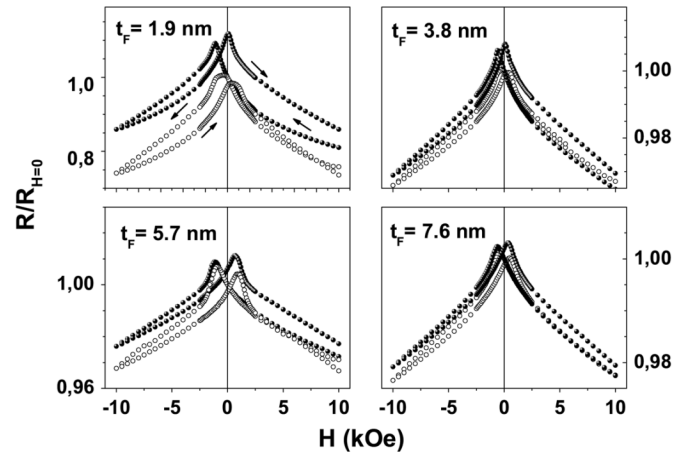


Fig. 2. Normalized AMR loops. $AF(7.6 \text{ nm})$ $T = 18$ K, $H_{FC} = 1$ T. FC (filled symbols) and ZFC (open symbols) loops show asymmetries between the two branches. Arrows indicate branches.

atomic plane resolution. We clearly observe the interface between the F-doped layers in the middle of two AF layers; the interfaces are sharp with interfacial roughness values around 0.38 nm (1 u.c.) in accordance with that extracted from XRD SUPREX refinement fit. It also shows a homogeneous strain along the interfaces of the superlattice. Statistical analysis of digitized atomic force microscope (AFM) images conducted on these superlattices yields surface roughness around 9 nm, for a $5 \times 5 \mu\text{m}^2$ image size. Assuming correlated roughness, the interfacial roughness ranges from 1 to 3 u.c.

It is well established that magnetoresistance measurements can be used to investigate exchange bias in thin films [5]. Resistance data were taken on a series of $[AF(7.6 \text{ nm})/F(t_F)]_N$ superlattices, cooling down from room temperature to approximately 50 K, either at zero applied field (ZFC) or during field cooling (FC) at 10 kOe. Both ZFC and FC $R(T)$ curves resemble the typical curves observed for individual F films [6]. Fig. 2 shows the isothermal FC and ZFC magnetoresistance loops taken at 15 K AMR, is normalized to the value obtained at $H = 0$. The loop exhibits asymmetries between the two (descending and ascending) branches, each indicated by arrows. The ZFC resistance has the maximum in the negative fields, for all measured

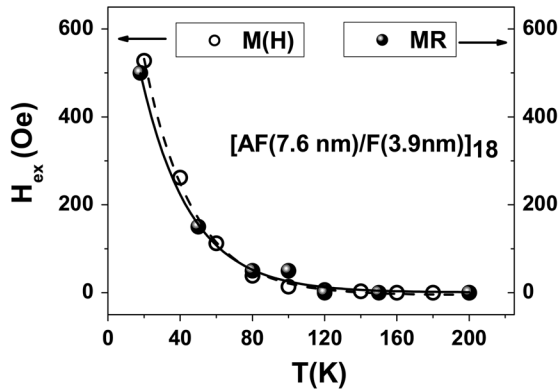


Fig. 3. H_{ex} , extracted from hysteresis loops (open symbols) and AMR data (filled symbols) for the $[\text{AF}(7.6 \text{ nm})/\text{F}(3.9 \text{ nm})]_{18}$ superlattice. Black lines show the fitting function.

multilayers, of the descending (from 1 to -1 kOe) fields. In the case of the FC curve, the resistance maximum appears in the positive field range of the ascending (from -10 to 10 kOe) field branch. On the other hand, for the FC loop, the position of the resistance maxima are not symmetric around the y axis at $H = 0$. In all samples a shift of the FC loop with respect to that of the ZFC along the field axis is observed. The shape of the AMR traces in Fig. 2 shows that the approach to saturation on each side of the loop is apparently the same. It is the reduction of the field from saturation, which shows asymmetry in the AMR, i.e., these measurements are sensitive to the initial stages of reversal. This process becomes sharper as the field is reduced from positive saturation, where magnetization reversal occurs by rotation, than when the field is reduced from negative saturation, where nucleation and propagation is the dominant mechanism, as has been shown by Leighton *et al.* [7]. The value of H_{ex} is determined from the displacement of the maximum in the AMR loops.

Fig. 3 plots the temperature dependence of H_{ex} from 15 to 200 K, for the $[\text{AF}(7.6 \text{ nm})/\text{F}(1.9 \text{ nm})]_{18}$ superlattice, open symbols. It is interesting to observe that H_{ex} follows an exponential decrease with temperature, similar to that found for H_{ex} extracted from isothermal magnetic hysteresis loops [8] for the same superlattice, which is also plotted in Fig. 3, left axis, filled symbols. Both experimental data can be fitted to an exponential decay expression:

$$H_{\text{ex}} = H_{\text{ex}}^0 \exp(-T/T_0) + C. \quad (1)$$

The lines in Fig. 3 correspond to the fit with (1). T_0 represents the energy barrier for thermal activation of the interfacial magnetization responsible for exchange bias. The FC magnetoresistance measurements confirm that the asymmetries found in the isothermal loops can be attributed to the effect of exchange biased AF/F manganite interfaces [3]. For all samples studied, H_{ex} drops to zero at around 150 K, which is higher than the

blocking temperature previously reported in [3] for these types of manganite superlattices (~ 80 K). Nevertheless, it is reasonably close to the Néel temperature T_N expected for these AF manganites. The parameters obtained from (1) can also be analyzed and correlated with the F thickness, which we do for a set of samples with constant t_{AF} at 7.6 nm, varying t_F : 1.9, 3.8, 5.7, and 7.6 nm. Interestingly, the T_0 parameter shows basically no change with increased F-layer thickness, being constant at approximately 29 ± 1 K. However, for this series of superlattices with a varied t_F and a constant t_{AF} , the H_{ex}^0 parameter increases for thinner F-layer thicknesses.

In summary, we grew high quality F-AF manganite superlattices, as indicated by XRD and TEM analysis. Isothermal FC-AMR curves for this series of superlattices show nonsymmetric positions of the resistance maximum that could be attributed to the exchange biasing mechanism present in these superlattices.

ACKNOWLEDGMENT

This work was supported by COLCIENCIAS under the Excellence Center for Novel Materials, Contract 043-2005. Work at Argonne National Laboratory was supported by U.S. DOE-BES under Contract W-31-109-ENG-38. Work at Centro Atómico Bariloche was supported in part by ANPCyT-PICT2003-03-13297.

REFERENCES

- [1] Y. Ijiri, "Coupling and interface effects in magnetic oxide superlattices," *J. Phys.: Condens. Matter*, vol. 14, pp. R947–R966, 2002.
- [2] J. Nogués and I. K. Schuller, "Exchange bias," *J. Magn. Magn. Mater.*, vol. 192, p. 203, 1999.
- [3] I. Panagiotopoulos, C. Christides, N. Moutis, M. Pissas, and D. Niarchos, "Exchange-biasing mechanism in $\text{La}_{2/3}\text{Ca}_{1/3}\text{MnO}_3/\text{La}_{1/3}\text{Ca}_{2/3}\text{MnO}_3$ multilayers," *Phys. Rev. B*, vol. 60, pp. 485–491, 1999.
- [4] E. E. Fullerton, I. K. Schuller, H. Vanderstraeten, and Y. Bruynseraede, "Structural refinement of superlattices from X-ray diffraction," *Phys. Rev. B*, vol. 45, p. 9292, 1992.
- [5] Y. Chen, D. K. Lottis, and E. D. Dahlberg, "Magnetic properties of Fe thin films," *J. Appl. Phys.*, vol. 70, p. 5822, 1991.
- [6] G. Campillo, L. F. Castro, P. Vivas, E. Baca, P. Prieto, D. Arias, J. Santamaría, A. Berger, and S. D. Bader, "Direct growth of epitaxial $\text{La}_{0.67}\text{Ca}_{0.33}\text{MnO}_3$ —Thin films," *Surf. Rev. Lett.*, vol. 9, pp. 1611–1615, 2002.
- [7] C. Leighton, M. Song, J. Nogués, M. C. Cyrille, and I. K. Schuller, "Using magnetoresistance to probe reversal asymmetry in exchange-biased bilayers," *J. Appl. Phys.*, vol. 88, p. 344, 2000.
- [8] P. Prieto, M. E. Gómez, G. Campillo, A. Berger, E. Baca, R. Escudero, F. Morales, J. Guimpel, and N. Haberkorn, "Exchange-coupling effect and magnetotransport properties in epitaxial $\text{La}_{2/3}\text{Ca}_{1/3}\text{MnO}_3/\text{La}_{1/3}\text{Ca}_{2/3}\text{MnO}_3$ superlattices," *Phys. Status Sol. (a)*, vol. 201, p. 2343, 2004.
- [9] R. L. Stamps, "Mechanisms for exchange bias," *J. Phys. D: Appl. Phys.*, vol. 33, pp. R247–R268, 2000.